Journal of Statistical Physics, Vol. 110, Nos. 3–6, March 2003 (© 2003)

Molecular Motor Cycles: From Ratchets to Networks[1]

Reinhard Lipowsky[2] and Nicole Jaster[2]

Received December 10, 2001; accepted May 2, 2002

Molecular motor cycles are studied in the framework of stochastic ratchets in which the motor moves along a 1-dimensional track, can attain M internal states, and can undergo transitions between these levels at K spatial positions. These ratchets can be mapped onto a stochastic network of KM discrete states. The network is governed by a Master equation, fulfills a vertex rule, and satisfies detailed balance in the absence of enzymatic activity and external force. Any pathway of the motor cycle which leads to a forward or backward step of the motor corresponds to a certain sequence of transitions spanning this network. The dependence of the motor velocity on the transition rates can be determined for arbitrary values of K and M and exhibits some simple and universal features.

KEY WORDS: molecular motor; motor cycle; stochastic ratchet; stochastic network; motor velocity.

1. INTRODUCTION

The transport of vesicles and other cargo in the living cell is based on molecular motors which move along cytoskeletal filaments. The movements of these motors involve several time regimes: (I) In the short time regime, the motor molecule undergoes a cycle of conformational changes which is coupled to ATP hydrolysis. This motor cycle leads to a single "power stroke" and, thus, to a single step along the filament. In the presence of a sufficient amount of ATP, the corresponding time scale is of the order of 10 milliseconds. This time scale increases with decreasing ATP concentration as soon as the process becomes limited by the diffusion of ATP molecules towards the motor; (II) In the intermediate time regime, the

[1] Dedicated to Michael E. Fisher on the occasion of his 70th birthday.

[2] MPI für Kolloid- und Grenzflächenforschung, D-14424 Potsdam, Germany; e-mail: lipowsky@mpikg-golm.mpg.de

0022-4715/03/0300-1141/0 © 2003 Plenum Publishing Corporation

motor stays bound to the filament and performs a directed walk along it. These walks typically consist of about a hundred steps along the filaments; and (III) In the long time regime, the motor undergoes random walks arising from many diffusional encounters between the motors and the filaments.

In this article, we study theoretical models for the motor cycle which governs the short time regime (I) and determine the corresponding transport properties for the directed walks of the motor in the intermediate time regime (II). These models, which we have introduced in previous work,[1–3] are stochastic ratchets equivalent to diffusion-reaction models or composite Markov processes, see, e.g., ref. 4, with space-dependent transition rates and represent generalizations of the two-state models considered in refs. 5–9. The stochastic ratchets are characterized (i) by a spatial coordinate x which describes the displacement of the motor molecule along the filament, (ii) by M internal states which represent the various conformations the molecule can attain for a fixed value of x, and (iii) by K spatial positions per motor cycle at which the motor molecule can undergo transitions between these different internal states. As reported in ref. 2, these ratchet models can be mapped onto stochastic networks with KM discrete states.

Motor cycles are often discussed using the terminology of biochemical reactions and enzyme kinetics. One then talks of kinetic pathways which are coupled to the conformational changes of the motor molecule. Here and below, we will use the term "pathway" to represent a cyclic sequence of molecular conformations which leads to a forward or backward step of the molecular motor along the filament. Within the network representation of the KM ratchets, each such pathway corresponds to a cyclic path which spans this network in the x-direction, i.e., in the spatial direction parallel to the filament.

The transport properties of bound motors in the intermediate time regime (II) have also been studied in many experiments. The most important property is their velocity which has been measured for several cytoskeletal motors such as two-headed kinesin,[10–18] one-headed kinesin,[19] myosin V,[20–22] and dynein[23–25] which move along microtubuli or actin filaments.

For two-headed kinesin, the motor velocity has been measured as a function of two control parameters. The first such parameter is provided by the ATP concentration Γ, i.e., by the concentration of the fuel molecules. The second control parameter is given by the external load force F which is usually applied by an optical trap. Several experiments have shown that the average motor velocity v increases monotonically with Γ and exhibits a saturation behavior. In addition, the data for zero or small F could be

fitted by the hyperbolic form $v(\Gamma) \simeq v_{\max}\Gamma/(\Gamma_* + \Gamma)$.[10, 12, 14] More recently, Visscher *et al.*[18] have found that such a fit is even possible over the whole range of accessible forces as given by $0 \leqslant |F| \leqslant 5.6$ pN provided one uses F-dependent fit parameters $v_{\max}$ and Γ_* which leads to

$$v(\Gamma, F) \simeq v_{\max}(F)\,\Gamma/[\Gamma_*(F)+\Gamma]. \tag{1.1}$$

This relation is reminiscent of the Michaelis–Menten relation for the rate of enzymatic reactions. An analogous relation has also been proposed for the experimental data on myosin V.[21, 22]

As shown in our previous work,[2, 3] the Michaelis–Menten-type relation as given by (1.1) represents the simplest relationship of a whole family of more general velocity-concentration relations. These more general relationships provide a *classification scheme* for the chemomechanical coupling of molecular motors. On the one hand, it follows from this scheme that the Michaelis–Menten-type relation (1.1) applies to motor cycles which exhibit the following simplifying features: (i) there is only a single pathway leading to a forward step, (ii) this pathway involves only one ATP hydrolysis which obeys Michaelis–Menten kinetics, and (iii) there are no pathways leading to backward steps. On the other hand, this classification scheme also shows that one will, in general, observe velocity-concentration relationships which *differ* from (1.1) as soon as (i) there is more than one possible pathway which leads to a forward step, or (ii) there is a pathway which involves more than one ATP hydrolysis, or (iii) there are pathways which lead to backward steps.

The force dependence of the two parameters $v_{\max}(F)$ and $\Gamma_*(F)$ in (1.1) reflects the molecular force potentials as discussed in ref. 1 for ratchet models and a variety of sawtooth potentials. More recently, Fisher and Kolomeisky[26] found that the force dependence as observed experimentally by Visscher *et al.*[18] can be understood in terms of discrete sequential models in which the motor steps along a linear track of discrete binding sites by passing through a sequence of intermediate states.[27, 28] The latter sequence represents a particular pathway of the motor molecule and, thus, should correspond to a certain cyclic path across the KM networks discussed here.

Our article is organized as follows. In Section 2, we will first define our general class of ratchet models as previously studied in refs. 1 and 2. As mentioned, the motor is described by M internal states and can undergo transitions at K spatial locations per motor cycle. When the spatially localized rates are parametrized by delta functions, these ratchet models can be mapped explicitly onto a network of KM discrete states as discussed in Section 3. A general algorithm to obtain the stationary states of these

networks is described in Section 4. The general classification scheme is discussed in Section 5 for the current-rate relationships and in Section 6 for the velocity-concentration relationships. The underlying ATP hydrolysis which keeps the system out of equilibrium is discussed in Section 6.1. In this latter section, we also discuss (i) the chemical equilibrium between ATP, ADP and inorganic phosphate, and (ii) the ADP concentration as a possible control parameter.

As mentioned, the possible pathways of the motor cycle correspond to certain closed paths which span these networks in the x-direction and represent cycles in the graph theoretic sense. This is explained in more detail at the beginning of Section 3, compare Fig. 2 below. In fact, the total current across the network can be decomposed in such a way that each contribution corresponds to a certain network-spanning cycle, see Section 5.1.

In the present article, we focus on the generic properties of the KM ratchets, which are valid for all values of M and K, and emphasize their representation in terms of stochastic networks. In a subsequent article,[29] we will discuss several specific examples of KM ratchets with $K \leqslant 4$ and $M \leqslant 4$.

2. STOCHASTIC RATCHET DYNAMICS

2.1. Time Evolution with M Internal States

Within the theoretical approach used here, the movement of the motor molecule along the filament is described by the spatial coordinate x. For cytoskeletal and other linear motors, one useful choice for x is the displacement of the center-of-mass of the motor parallel to the filament. A similar approach should apply to rotary motors where x would represent an appropriate angular coordinate.

For a given value of x, the motor molecule must be bound to the filament but can still attain many different conformations. These different internal states will be labeled by the discrete index m with $m = 1, 2, \ldots, M$. In addition, the motor can undergo transitions between these states at a discrete set of K spatial positions per motor cycle.

Depending on the molecular architecture of the motor, one may identify several discrete subgroups of internal states. If the motor has only one enzymatic domain or head, this head can attain a discrete number of states corresponding to (i) no substrate, (ii) adsorbed ATP, (iii) adsorbed ADP/P, and (iv) adsorbed ADP. In each of these states, the motor may adopt a different conformation which will experience different interactions with the filament. If the motor has two heads, a and b, one has three

groups of internal states corresponding to (I) two bound heads, (II) bound head *a*, and (III) bound head *b*.

In general, the motor conformation also involves internal degress of freedom which vary in a continuous fashion. For example, one may tilt a two-headed motor molecule, which is bound by one head, and simultaneously move its unbound head without changing the position of its center-of-mass. In the theoretical framework considered here, these continuous degrees of freedom are also discretized. On the one hand, this is convenient from a computational point of view. On the other hand, such a discretization does not represent a real limitation compared to a continuous description (such as the one proposed in ref. 30, for example) since one may include many intermediate states by choosing a sufficiently large value of M.

The stochastic dynamics of the molecular motor is now described by the probability densities $P_m(x, t)$ to find the motor at position x and in the internal state m. For a given position x, the densities P_m may change (i) because of lateral diffusion in state m which leads to lateral currents J_m or (ii) because of transitions between the different internal states. Therefore, the probability densities P_m satisfy the continuity equations

$$\partial P_m(x, t)/\partial t + \partial J_m(x, t)/\partial x = I_m(x, t) \tag{2.1}$$

with the transition current densities I_m. In order to discuss the formal properties of these equations, it will be convenient to visualize the M internal states as M levels. In the following, the terms "internal state" and "level" are synonymous.

The lateral currents J_m depend on the molecular interaction potentials $U_m(x)$ and on the external force F which define the effective force potentials

$$V_m(x) \equiv [U_m(x) - Fx]/T \tag{2.2}$$

where T is the temperature in energy units. As mentioned, the subscript m labels the different internal states of the motor corresponding to the different conformations of the motor molecule for fixed value of x. Now, assume that we "freeze" the motor in a specific conformation corresponding to a certain value of m and that we displace this "frozen" state along the filament. At position x, the motor molecule will then feel the force $-\partial U_m(x)/\partial x$ arising from its interactions with the filament.

We will assume that the x-dependence of the molecular interaction potentials $U_m(x)$ exhibits a characteristic length scale denoted by ℓ. In fact, we will focus on periodic potentials for which ℓ represents the potential period and $U_m(x+\ell) = U_m(x)$.

Using the effective force potentials defined by (2.2), the lateral currents J_m have the Smoluchowski– or Fokker–Planck form[31, 4]

$$J_m(x,t) \equiv -D_m \left[\frac{\partial}{\partial x} V_m(x) + \frac{\partial}{\partial x} \right] P_m(x,t)$$

$$= -D_m e^{-V_m(x)} \frac{\partial}{\partial x} [e^{V_m(x)} P_m(x,t)]. \tag{2.3}$$

where the parameter D_m represents the small-scale diffusion coefficient in level m. The corresponding friction coefficients are given by T/D_m as follows from the Einstein relation. This generalizes the ratchet models studied in refs. 1 and 2 where all levels were taken to have the same friction coefficient.

The transition current densities I_m depend on the transition rate functions $\Omega_{mn} = \Omega_{mn}(x) \geqslant 0$ from state m to state n and have the generic form

$$I_m(x,t) \equiv \sum_n{}' [-P_m(x,t)\, \Omega_{mn}(x) + P_n(x,t)\, \Omega_{nm}(x)] \tag{2.4}$$

where the prime at the summation sign indicates that n is restricted to $n \neq m$.

Summation of (2.4) over m leads to $\sum_m I_m(x,t) = 0$ since the double sum over m and n contains each term twice and with opposite sign. It then follows from the sum over the M continuity equations for P_m as given by (2.1) that the position probability density $P_{\text{tot}} \equiv \sum_m P_m$ evolves according to

$$\partial P_{\text{tot}}(x,t)/\partial t + \partial J_{\text{tot}}(x,t)/\partial x = \sum_m I_m(x,t) = 0. \tag{2.5}$$

with the total lateral current $J_{\text{tot}}(x,t) \equiv \sum_m J_m(x,t)$. The latter equation is obvious since we implicitly assume that the motor stays bound to the filament. Therefore, in the present situation, the probability to find the motor in a bound state is conserved.

Real molecular motors detach from the filament after a certain number of motor cycles and then undergo random walks which consist of alternating sequences of bound and unbound motor states, i.e., of directed walks along the filaments and nondirected diffusion in the aqueous solution. The properties of these walks, which will not be considered here, have been studied in refs. 32–35.

2.2. Transitions at K Spatial Locations

As mentioned in the introduction, stochastic models of the form as given by (2.1)–(2.4) have been primarily studied for transition rate functions

Ω_{mn} which do not depend on the spatial coordinate x.[4] In contrast, we will focus here on the case for which these transition rate functions are spatially localized as recently studied in the context of molecular motors.[8, 1, 2]

Thus, the transition rate functions are assumed to be localized in space at the discrete set of positions $x = x_k$ with $k = 1,\ldots, K$ and $0 \leqslant x_1 < \cdots < x_K < \ell$ and are expressed as[1, 2]

$$\Omega_{mn}(x) \equiv \sum_k \omega_{mn}(x_k)\, \ell_\Omega\, \delta(x - x_k) \tag{2.6}$$

where $\omega_{mn}(x_k) \geqslant 0$ are transition rates, $\ell_\Omega \ll \ell$ represents a molecular "localization" length, and $\delta(z)$ is Dirac's delta function. The parametrization (2.6) in terms of delta functions is useful since the ratchet models can then be solved analytically as described in Section 3.

2.3. Stationary States

We will now focus on stationary states for which the probability densities P_m satisfy $\partial P_m/\partial t = 0$ which implies $\partial P/\partial t = 0$ for the position probability density P. It then follows from the continuity equation (2.5) for P that the total lateral current $J_{\text{tot}} = \sum_m J_m = \text{const}$.

For such a stationary state, integration of the expressions (2.3) for the lateral currents J_m leads to

$$P_m(x) = P_m(x_*)\, e(x_*, m \mid x, m) - \frac{1}{D_m} \int_{x_*}^{x} dy\, J_m(y)\, e(y, m \mid x, m) \tag{2.7}$$

with the exponential functions

$$e(x, m \mid y, n) \equiv \exp[V_m(x) - V_n(y)] = 1/e(y, n \mid x, m) \tag{2.8}$$

which depend on the effective force potentials $V_m(x) = [U_m(x) - Fx]/T$ as defined in (2.2). Note that all exponential functions which enter in (2.7) have $n = m$ which implies that this equation is not affected by the substitution $V_m(x) \to V_m(x) + c_m$ with x-independent terms c_m. The exponential functions defined in (2.8) satisfy the simple product rule

$$e(x_1, m \mid x_2, m)\, e(x_2, m \mid x_3, m) = e(x_1, m \mid x_3, m). \tag{2.9}$$

Further below, we will evaluate the general relation (2.7) for various choices of x and x_*.

In order to have a well-defined stationary state, we will consider the finite interval $0 \leqslant x < \ell$ and use periodic boundary conditions with the "box normalization"

$$\int_{x_1}^{x_1+\ell} dx\, P_{\rm tot}(x) = \int_{x_1}^{x_1+\ell} dx \sum_m P_m(x) \equiv 1 \tag{2.10}$$

which implies one motor particle per box and, thus, the motor velocity $v = \ell J_{\rm tot}$. This normalization is particularly convenient for periodic potentials $U_m(x)$ for which the box size is identified with the potential period and $U_m(x+\ell) = U_m(x)$.

2.4. Detailed Balance

If there is no enzymatic activity and the applied force $F = 0$, the system must obey detailed balance (db). This implies that the probability densities $P_m(x) = P_m^{db}(x)$ and the transition rate functions $\Omega_{mn}(x) = \Omega_{mn}^{db}(x)$ satisfy

$$P_m^{db}(x)\, \Omega_{mn}^{db}(x) = P_n^{db}(x)\, \Omega_{nm}^{db}(x). \tag{2.11}$$

Thus, the transition current density as given by (2.4) is identically zero and all levels are decoupled. Furthermore, the current $J_m = J_m^{db}$ must also vanish for each level m since $F = 0$ and there is no coupling to another level. It then follows from the expression (2.3) for the lateral currents that $P_m(x) \sim \exp[-U_m(x)/T]$ which is the usual Boltzmann weight for the equilibrium distribution. Finally, insertion of this Boltzmann weight into (2.11), leads to the relation

$$\Omega_{mn}^{db}(x) = e^{[U_m(x) - U_n(x)]/T} \Omega_{nm}^{db}(x) = e^{V_m(x) - V_n(x)} \Omega_{nm}^{db}(x). \tag{2.12}$$

When the transition rate functions are localized and parametrized as in (2.6), the corresponding transition rates $\omega_{mn}(x_k) = \omega_{mn}^{db}(x_k)$ satisfy[2]

$$\omega_{mn}^{db}(x_k) = e^{V_m(x_k) - V_n(x_k)} \omega_{nm}^{db}(x_k) = e(x_k, m \mid x_k, n)\, \omega_{nm}^{db}(x_k) \tag{2.13}$$

where the exponential function $e(x, m \mid y, n)$ has been defined in (2.8).

In order to emphasize the deviations from detailed balance, the transition rates $\omega_{mn}(x_k)$ will now be divided up according to

$$\omega_{mn}(x_k) = \omega_{mn}^{db}(x_k) + \Delta_{mn}(x_k) \tag{2.14}$$

with the balanced parts ω_{mn}^{db} and the unbalanced parts Δ_{mn} arising from the enzymatic activity.

It is instructive to consider the case of no enzymatic activity but finite external force $F \neq 0$. Since $V_m(x) = [U_m(x) - Fx]/T$, the force F drops out from the prefactor $\exp[V_m(x) - V_n(x)]$ in the detailed balance relation (2.12). Thus, one might be tempted to conclude from (2.3) that the probability distribution is now given by $P_m(x) \sim \exp[-V_m(x)]$. This solution is, however, not acceptable since (i) it would imply the unphysical result $J_m = 0$ and (ii) it does not fulfill the periodic boundary conditions. In contrast, the physically acceptable solution must have the same periodicity as the underlying molecular potentials[31] and must, in general, lead to a finite lateral current $J_m \neq 0$.

3. STOCHASTIC NETWORK AND MASTER EQUATION

We will now show that the stationary states of the stochastic dynamics as defined in the previous section can be reduced to a set of relations between the probabilities $P_m(x_k)$, i.e., between the probabilities to find the motor at position $x = x_k$ in level m. Thus, we will reduce the dynamics to a discrete set of KM motor states labeled by (k, m). It is further convenient to represent this discrete set of states in terms of a network of vertices, again denoted by (k, m), see Fig. 1. These discrete states are connected by directed edges or di-edges which represent local transition currents between the states. The form of these transition currents will be determined in the next subsections.

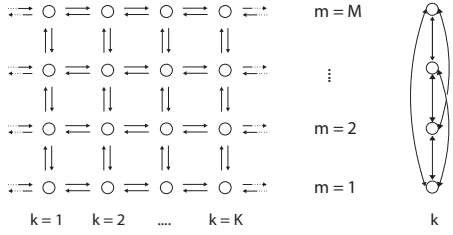

Fig. 1. Network of discrete motor states represented by vertices (k, m) with $1 \leqslant k \leqslant K$ and $1 \leqslant m \leqslant M$. For fixed m, each pair of adjacent locations k and $k+1$ is connected by a pair of horizontal di-edges (i.e., directed edges). Since the network is periodic in the horizontal direction, the first column with $k = 1$ and the last column with $k = K$ are also connected as indicated by the broken di-edges. For fixed k, each pair of internal states, m and m', is connected by a pair of vertical di-edges. In the graph on the left, only a subset of all vertical di-edges is shown for simplicty. In the graph on the right, all vertical di-edges are indicated for one value of k.

The network shown in the left part of Fig. 1 looks 2-dimensional but each vertex (k, m) is connected to $M-1$ other vertices (k, m') at the same x-position and to the two vertices $(k-1, m)$ and $(k+1, m)$. Since M can be large, any finite lattice with any dimensionality $d = 1 + d_\perp$ can be mapped onto such a network. The periodic boundary conditions in the x-direction imply a pair of di-edges between the vertices $(k = 1, m)$ and $(k = K, m)$ for all values of m.

At this point, it is useful to view the network shown in Fig. 1 as a directed graph and to borrow some elementary concepts from graph theory.[36] Thus, we define a *walk* in the network to consist of a sequence of vertices where each subsequent pair of vertices is connected by a di-edge contained in the network. Furthermore a *path* in the network is a walk for which no vertex occurs twice, and a *cycle* is a closed path.

Because of the periodic boundary conditions, any path which starts at vertex $(k = 1, m)$, spans the whole network parallel to the x-direction, and ends at vertex $(k = K, m)$, compare Fig. 2, can be completed to a cycle if one adds the di-edge between $(k = K, m)$ and $(k = 1, m)$. We will refer to these cycles as positive s-cycles since they traverse the network in the positive x-direction (the prefix "s" stands for "spanning"). Cycles which traverse the network in the opposite direction will be called negative s-cycles, see Fig. 2.

In the biochemical literature, one usually refers to the main pathway of an enzyme which is often drawn as a cycle of chemical reactions. In the present context of molecular motors, various schemes for such a main pathway have been proposed, see, e.g., ref. 37. Within the theoretical framework described here, the main pathway should be identified with that positive s-cycle which carries the largest current, for each value of x, across the network. In general, this sequence need not be unique. Indeed, any positive or negative s-cycle of the network corresponds to a possible pathway which leads to a forward or backward motor step, respectively.

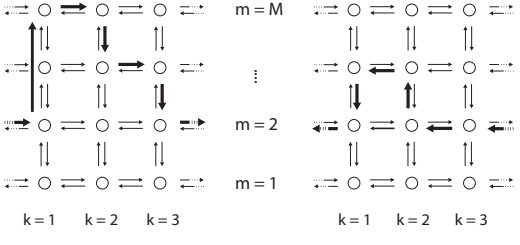

Fig. 2. Spanning cycles or s-cycles in the directed graph of the network as indicated by the sequences of thick arrows: (left) Positive s-cycle and (right) Negative s-cycle spanning the network in the positive and negative x-direction, respecitively.

3.1. Local Currents

The spatially localized transition rate functions as given by (2.6) imply relatively simple expressions for the local currents between the different states (k, m). In order to show this, we first define the local transition current

$$J_{mn}(x_k) \equiv P_m(x_k)\, \omega_{mn}(x_k)\, \ell_\Omega \geqslant 0 \tag{3.1}$$

which represents the current from state (k, m) to state (k, n). Likewise, the transition current from state (k, n) to state (k, m) is given by $J_{nm}(x_k)$. These two currents correspond to a pair of di-edges which connect the two vertices (k, m) and (k, n) and which have a vertical orientation in Fig. 1. The *total* current which flows from (k, m) to (k, n) is equal to $J_{mn}(x_k) - J_{nm}(x_k)$.

In order to obtain expressions for the lateral currents $J_m(x)$, we insert the localized transition rate functions (2.6) into the current densities I_m as in (2.4) and integrate the continuity equation $\partial J_m / \partial x = I_m$. This leads to

$$J_m(x) = \bar{J}_m + \sum_{k=1}^{K} \Delta J_m(x_k)\, \theta(x - x_k) \tag{3.2}$$

with x-independent coefficients $\bar{J}_m$ and the current discontinuities

$$\Delta J_m(x_k) \equiv \sum_n{}' \left[-J_{mn}(x_k) + J_{nm}(x_k) \right] \tag{3.3}$$

where $\theta(x)$ is Heaviside's step function with $\theta(x) = 0$ for $x < 0$ and $\theta(x) = 1$ for $x > 0$. As before, the prime at the summation sign indicates that n is restricted to $n \neq m$.

Note that $\sum_m \Delta J_m(x_k) = 0$ for all x_k since the double sum over m and n again contains each term twice and with opposite sign. Therefore, summation of (3.2) over m leads to the total lateral current $J_{\text{tot}} = \sum_m J_m = \sum_m \bar{J}_m$.

The currents $J_m(x)$ as given by (3.2) are piece-wise constant functions of x. It follows by direct inspection of this equation that the lateral current $J_m(x_k, x_{k+1})$ from state (k, m) to state $(k+1, m)$ is given by

$$\begin{aligned} J_m(x_k, x_{k+1}) &= \bar{J}_m + \sum_{q=1}^{k} \Delta J_m(x_q) \\ &= \bar{J}_m + \sum_{q=1}^{k} \sum_n{}' \left[-J_{mn}(x_q) + J_{nm}(x_q) \right] \end{aligned} \tag{3.4}$$

which is equivalent to

$$J_m(x_k, x_{k+1}) = J_m(x_{k-1}, x_k) + \sum_n{}' \left[-J_{mn}(x_k) + J_{nm}(x_k) \right]. \tag{3.5}$$

The relation as given by (3.5) represents a conservation law for all local currents connected to a given state (k, m). In order to visualize this relation, we will now divide the lateral currents $J_m(x_k, x_{k+1})$ into two contributions, one for the current from (k, m) to $(k+1, m)$ and another one for the current in the opposite direction from $(k+1, m)$ to (k, m). In order to do this, we start from the general relations (2.7) which express the probability densities P_m in terms of the currents J_m. Using (2.7) with the choice $x = x_{k+1}$ and $x_* = x_k$ with $k = 1, 2, \ldots, K-1$, one finds

$$J_m(x_k, x_{k+1}) = P_m(x_k) \frac{e_m(x_k, x_{k+1})}{\mathscr{E}_m(x_k, x_{k+1})} - P_m(x_{k+1}) \frac{1}{\mathscr{E}_m(x_k, x_{k+1})} \tag{3.6}$$

with the $\mathscr{E}$-functions

$$\mathscr{E}_m(x, y) \equiv \frac{1}{D_m} \int_x^y dz\, e_m(z, y) = \frac{1}{D_m} \int_x^y dz \exp[V_m(z) - V_m(y)]. \tag{3.7}$$

The first term in (3.6) corresponds to the transition current from state (k, m) to state $(k+1, m)$, the second term to the current from $(k+1, m)$ to (k, m). In Fig. 1, these two transition currents are drawn as a pair of horizontal di-edges.

The $\mathscr{E}$-functions as given by (3.7) depend on the molecular force potentials $U_m(x)$ and on the applied force F via the effective force potentials $V_m(x) = [U_m(x) - Fx]/T$. Note that $\mathscr{E}_m(x, y) \geqslant 0$ for all values of x and y with $x < y$.

3.2. Vertex Rule

At this point, it is useful to introduce a somewhat different notation. First, the probabilities to find the motor in the discrete states (k, m) are now denoted by

$$P(k, m) \equiv P_m(x_k)\, \ell_\Omega \tag{3.8}$$

where we used the localization length ℓ_Ω to make $P(k, m)$ dimensionless. Secondly, we introduce the forward transition rate

$$W(k, m \,|\, k+1, m) \equiv \frac{e_m(x_k, x_{k+1})}{\mathscr{E}_m(x_k, x_{k+1})\, \ell_\Omega} \tag{3.9}$$

and the backward rate

$$W(k+1, m \mid k, m) \equiv \frac{1}{\mathscr{E}_m(x_k, x_{k+1})\, \ell_\Omega} \tag{3.10}$$

Using these definitions, the relation (3.6) for the lateral currents becomes

$$J_m(x_k, x_{k+1}) = P(k, m)\, W(k, m \mid k+1, m) - P(k+1, m)\, W(k+1, m \mid k, m) \tag{3.11}$$

Likewise, we rewrite the interlevel current $J_{mn}(x_k)$ as given by (3.1) in the form

$$J_{mn}(x_k) \equiv P(k, m)\, W(k, m \mid k, n) \tag{3.12}$$

with

$$W(k, m \mid k, n) \equiv \omega_{mn}(x_k) \tag{3.13}$$

Finally, insertion of these relations into the local conservation law (3.5) leads to

$$\begin{aligned} 0 = \sum_n{}' \, & [-P(k, m)\, W(k, m \mid k, n) + P(k, n)\, W(k, n \mid k, m)] \\ & - P(k, m)\, W(k, m \mid k+1, m) + P(k+1, m)\, W(k+1, m \mid k, m) \\ & - P(k, m)\, W(k, m \mid k-1, m) + P(k-1, m)\, W(k-1, m \mid k, m). \end{aligned} \tag{3.14}$$

The terms with a minus sign are the transition currents which flow *out of* the state (k, m), those with a plus sign are the currents which flow *into* this state. For the network representation in Fig. 1, this implies the vertex rule that, at each vertex (k, m), the sum of all outgoing currents, represented by di-edges pointing away from the vertex, is equal to the sum of all incoming currents, represented by di-edges pointing towards the vertex. This vertex rule resembles Kirchhoff's first rule for electric circuits.

3.3. Equivalent Master Equation

Inspection of the vertex rule as given by (3.14) shows that it has the same form as the the transition matrix of a Master equation. Indeed, the

stationary solutions for the stochastic ratchets considered here are identical to the stationary solutions of the Master equation as given by

$$\begin{aligned}\partial P(k,m)/\partial t = \sum_n{}' \, [&- P(k,m)\, W(k,m \mid k,n) + P(k,n)\, W(k,n \mid k,m)] \\ &- P(k,m)\, W(k,m \mid k+1,m) + P(k+1,m)\, W(k+1,m \mid k,m) \\ &- P(k,m)\, W(k,m \mid k-1,m) + P(k-1,m)\, W(k-1,m \mid k,m).\end{aligned} \tag{3.15}$$

which describes the temporal change of the probability to find the motor in state (k, m) in terms of the various transition currents.

In this way, the ratchet dynamics is shown to be equivalent to the stochastic network of KM discrete states. As explained in the previous subsection, all transition rates W of the network which enter in the Master equation (3.15) can be calculated in terms of the parameters of the underlying Fokker–Planck dynamics defined in Section 2. Detailed balance again applies for $F = 0$ and for the balanced transition rates $W(k, m \mid k, n) = W^{db}(k, m \mid k, n) \equiv \omega^{db}_{mn}(x_k)$. Using the definitions (3.9) and (3.10) for the forward and backward rates $W(k, m \mid k+1, m)$ and $W(k+1, m \mid k, m)$, it is easy to check that each pair of terms in (3.15), which corresponds to a pair of di-edges connecting the same pair of vertices in the network, cancels separately.

Finally, one should note that the representation of the dynamics in terms of a Master equation has another advantage: such a representation is rather convenient in order to study the dynamics by numerical methods.

4. SOLUTION PROCEDURE FOR GENERAL *K* AND *M*

4.1. Transfer Matrix and Linear Algebra

The stochastic network described in the previous section has two simplifying features: the x coordinate is 1-dimensional and satisfies periodic boundary conditions. The first property can be used in order to define a transfer matrix which relates the states at x_k with the states at x_{k+1}. More precisely, the conservation law for the local currents as given by (3.5) and the expression (3.6) for the lateral currents can be rewritten into a recursion relation of the form

$$[J(x_k, x_{k+1}), P(x_{k+1})] = [J(x_{k-1}, x_k), P(x_k)]\, \mathbf{T}(x_k, x_{k+1}) \tag{4.1}$$

where $[J, P] \equiv [J_1,..., J_M, P_1,..., P_M]$ is a row vector with $2M$ components and $\mathbf{T}$ is a $2M \times 2M$ transfer matrix.

The recursion relation (4.1) can be used in order to express all lateral currents and all probability densities in terms of the densities $P_m(x_1)$ and the lateral currents $\bar{J}_m$ which enter the system from $x < x_1$, see (3.2). Thus, in order to solve the problem, we need a set of $2M$ equations for the $2M$ unknowns $\bar{J}_m$ and $P_m(x_1)$.

$2M-1$ of these equations can be constructed using the periodic boundary conditions (PBCs). First, we obtain $M-1$ linear and homogeneous equations from the PBCs for $M-1$ of the M lateral currents $J_m(x)$. As mentioned, $\sum_m \Delta J_m(x_k) = 0$ for any value of x_k which makes one of the M PBCs linearly dependent on the other $M-1$. Secondly, the PBCs for the M densities $P_m(x)$ provide another set of M linear and homogeneous equations. Finally, one linear but inhomogeneous equation is obtained from the normalization condition (2.10). This set of $2M$ linear equations may be written in the form

$$[\bar{J}, P(x_1)]\,\mathbf{A} = [\bar{J}_1,..., \bar{J}_M, P_1(x_1),..., P_M(x_1)]\,\mathbf{A} = [0,..., 0, 1] \tag{4.2}$$

which defines the $2M \times 2M$ matrix $\mathbf{A}$. Each of the first $M-1$ columns of $\mathbf{A}$ corresponds to the PBC for one lateral current J_m, each of the next M columns to the PBC for one density P_m, and the $2M$th column to the normalization condition. The solution of (4.2) is given by

$$[\bar{J}, P(x_1)] = [0,..., 0, 1]\,\mathbf{A}^{-1} = [0,..., 0, 1]\,\frac{\mathbf{C}}{\det \mathbf{A}} \tag{4.3}$$

where the matrix elements of $\mathbf{C}$ are the cofactors

$$C_{ij} \equiv (-1)^{i+j} \det \mathbf{A}[j, i] \tag{4.4}$$

and $\mathbf{A}[i, j]$ is the $(2M-1) \times (2M-1)$ matrix obtained from $\mathbf{A}$ by erasing its ith row and jth column.

Finally, we want to calculate the total current $J_{\text{tot}} = \sum_{m=1}^{M} \bar{J}_m$ which determines the motor velocity v via $v = \ell J_{\text{tot}}$. It now follows from (4.3) and (4.4) that

$$J_{\text{tot}} = \sum_{m=1}^{M} \bar{J}_m = \sum_{m=1}^{M} (-1)^{2M+m} \det \mathbf{A}[m, 2M]/\det \mathbf{A}. \tag{4.5}$$

Note that the total current must not depend on the labeling of the discrete set of states. Thus, it must be invariant (i) if we permute the labels

m for the M levels and (ii) if we shift the labels k of x_k by any integer using the PBCs $x_{K+1} = x_1$.

4.2. Dependence on the Transition Rates

A detailed study of the linear set of equations reveals that one can make some general statements about the dependence of the matrix **A** on the transition rates $\omega_{mn}(x_k)$. The properties of **A** imply related properties of its determinant, its cofactors, and the total current as given by (4.5). All of these properties can be summarized in the following set of rules.

(A1): All matrix elements of **A**, which depend on $\omega_{mn}(x_1)$, are located in the $(M+m)$th row of **A** and are linear in $\omega_{mn}(x_1)$. This follows from the observation that $\omega_{mn}(x_1)$ enters the problem only via the product $P_m(x_1)\,\omega_{mn}(x_1)$, compare (3.1). This immediately implies the next rule

(A2): The determinant $\det \mathbf{A}$ and the cofactors $C_{ij} \sim \det \mathbf{A}[j, i]$ are *multilinear* in the transition rates $\omega_{mn}(x_1)$. This together with the relabeling invariance of the total current (4.5) implies

(A3): Both the determinant $\det \mathbf{A}$ and the cofactor sum

$$\sum_{m=1}^{M} (-1)^{2M+m} \quad \det \mathbf{A}[m, 2M] \tag{4.6}$$

are multilinear in the transition rates $\omega_{mn}(x_k)$ for *all* k.

(A4): All matrix elements of **A** which depend on $\omega_{mn}(x_K)$ are located in the two columns of **A** corresponding to the two PBCs for J_m and J_n. This follows from the observation that the reduction to the $2M$ variables $\bar{J}_m$ and $P_m(x_1)$ can be achieved by $(K-1)$ transfer matrixes $\mathbf{T}(x_k, x_{k+1})$ with $k \neq K$. Futhermore, for any pair of m and n, one may choose a set of $(M-1)$ PBCs which does *not* contain the PBC for J_n. For this choice, all matrix elements which depend on $\omega_{mn}(x_K)$ are located in the mth column; and

(A5): All terms occuring in the first $(M-1)$ columns of **A** are proportional to at least one transition rate $\omega_{mn}(x_k)$. As mentioned, the mth column corresponds to a PBC for the lateral current J_m which can be expressed in terms of the current discontinuities $\Delta J_m(x_k)$ according to

$$\sum_{k=1}^{K} \Delta J_m(x_k)/\ell_\Omega = \sum_{k=1}^{K} \sum_{n}{}' \left[-P_m(x_k)\,\omega_{mn}(x_k) + P_n(x_k)\,\omega_{nm}(x_k) \right] = 0. \tag{4.7}$$

Inspection of this equation shows that each term is proportional to at least one transition rate which implies the rule (A5).

5. UNIVERSAL FEATURES OF TOTAL CURRENT

5.1. Transition Rate Dependence of Total Current

Using the properties (A1)–(A5) as described in the previous section, one finds that the functional relationship between the total current J_{tot} and the transition rates $\omega_{mn}(x_k)$ exhibits some generic or universal features. In order to discuss these features, it will be often convenient to use the shorthand notation

$$\omega_r \quad \text{with} \quad 1 \leqslant r \leqslant N \equiv KM(M-1) \tag{5.1}$$

for $\omega_{mn}(x_k)$. The parameter N is equal to the number of all vertical di-edges in the network of KM discrete states as shown in Fig. 1.

The generic features of the current-rate relationship can be summarized in terms of the following rules:

Rule 0. The dependence of the total current J_{tot} on the transition rates ω_r has the form

$$J_{\text{tot}} = \frac{\text{Pol}_1(\omega_1, \omega_2, \ldots, \omega_N)}{\text{Pol}_2(\omega_1, \omega_2, \ldots, \omega_N)} \tag{5.2}$$

with two polynomials Pol_1 and Pol_2. This follows from (4.5) since the determinants are polynomials in the matrix elements of **A**, and each of these matrix elements can contain products of the transition rates.

Rule 1. Both polynomials are *multilinear* in all ω_r, i.e., each term $\mathscr{T}$ of both Pol_1 and Pol_2 behaves as

$$\mathscr{T} \sim \omega_1^{z_1} \omega_2^{z_2} \cdots \omega_N^{z_N} \qquad \text{with} \quad z_r = 0, 1, \tag{5.3}$$

i.e., it cannot contain powers ω_r^z with $z \geqslant 2$. This follows from (A3) when used in the expression (4.5) for the total current.

Rule 2. Each polynomial term $\mathscr{T}$ contains *at least* $M-1$ factors ω_r, i.e.,

$$\sum_r z_r \geqslant M-1 \qquad \text{for each } \mathscr{T}. \tag{5.4}$$

This follows directly from (A5). Furthermore, each polynomial term $\mathscr{T}$ contains at most $K(M-1)$ factors ω_r, i.e.,

$$\sum_r z_r \leqslant K(M-1) \qquad \text{for each } \mathscr{T}. \tag{5.5}$$

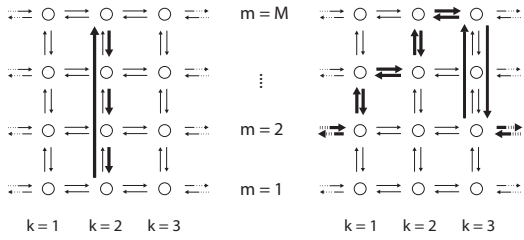

Fig. 3. (Left) A localized cycle or l-cycle at $k = 2$ which does not contribute, compare rule 4 in the text; and (Right) Pair of opposite s-cycles: These two s-cycles correspond to two terms in Pol_1 which cancel if the system satisfies detailed balance, see rule 6 in the text.

This follows directly from the next two rules 3 and 4. Note that this maximal number $K(M-1) = N/M$ grows as $\sim M$ whereas the total number $N = KM(M-1)$ of all rates ω_r grows as $\sim M^2$ for large M.

Rule 3. No term $\mathscr{T}$ contains a product of the form $\omega_{mn}(x_k)\,\omega_{mo}(x_k)$. This follows directly from (A1).

As defined at the beginning of Section 3, a cycle in the directed graph of the network is a closed walk for which no vertex occurs twice. In order to state the next rule, we define localized cycles or l-cycles to be those cycles for which all vertices have the same x-position and, thus, the same value of k, see the left graph in Fig. 3.

Rule 4. No term $\mathscr{T}$ contains a product of the form $\omega_{mn}(x_k)\,\omega_{nm}(x_k)$. This follows directly from (A4). Such a product corresponds to the smallest possible l-cycle. Likewise, no term $\mathscr{T}$ contains a product of the form

$$\omega_{mm'}(x_k)\,\omega_{m'm''}(x_k)\cdots\omega_{nm}(x_k). \tag{5.6}$$

The latter products correspond to all possible l-cycles at $x = x_k$ with $1 \leqslant k \leqslant K$.

At the beginning of Section 3, we introduced the notion of s-cycles spanning the whole network, see Fig. 2. First, note that l-cycles cannot occur within s-cycles; indeed, if an l-cycle were contained in an s-cycle, one vertex would occur twice in the s-cycle which is not possible by definition. Furthermore, there is a direct connection between s-cycles and the terms of Pol_1 as provided by the next rule.

Rule 5. For $F = 0$, each term $\mathscr{T}$ of Pol_1 can be mapped onto an s-cycle of the network. In general, this mapping is not one-to-one and several terms will be mapped onto the same s-cycle. The smallest such s-cycles involve a pair of transitions which connect two levels in opposite

directions at two different x-locations. The latter s-cycles lead to polynomial terms of the form

$$\mathcal{T} \sim \omega_{mn}(x_k)\, \omega_{nm}(x_l) \qquad \text{with} \quad k \neq l. \tag{5.7}$$

The latter rule can be deduced from the limiting case of detailed balance which is stated next.

Rule 6. If all transition rates satisfy detailed balance with $\omega_r = \omega_r^{db}$ as in (2.13), one has

$$J_{\text{tot}} \sim \text{Pol}_1(\omega_1^{db}, \omega_2^{db}, \ldots) = 0 \qquad \text{for} \quad F = 0. \tag{5.8}$$

In fact, each term of Pol_1 corresponding to a certain s-cycle is cancelled by another term corresponding to the opposite s-cycle, i.e., to the cycle which consists of the same vertices but has the opposite orientation, see the right graph in Fig. 3. This pair-wise cancellation is based on the exponential functions $e(x, m \mid y, n)$ as defined in (2.8) which enter (i) via the expressions (3.6) for the lateral currents and (ii) via the relation (2.13) for the balanced transition rates $\omega_{nm}^{db}(x_k)$.

The above set of rules 1–6 has been previously reported in ref. 2. In the present article, rule 2 has been extended and now contains the upper bound (5.5), rule 4 has been generalized to arbitrary l-cycles, see (5.6), and rules 5 and 6 have been stated in a more explicit form.

5.2. Dependence on Unbalanced Transition Rates

Since the balanced transitions do not contribute to the total current, let us now focus on the *unbalanced* transitions which have rates of the form

$$\omega_{mn}(x_k) = \omega_{mn}^{db}(x_k) + \Delta_{mn}(x_k) \qquad \text{with} \quad \Delta_{mn}(x_k) > 0 \tag{5.9}$$

as introduced in (2.14) or, using our short hand notation,

$$\omega_r = \omega_r^{db} + \Delta_r \qquad \text{with} \quad \Delta_r > 0. \tag{5.10}$$

The total number of such unbalanced transitions per motor cycle will be denoted by Q which satisfies the obvious inequality

$$Q \leqslant N = KM(M-1). \tag{5.11}$$

The simplest nontrivial network corresponds to $(K, M) = (2, 2)$ for which one has $Q \leqslant 4$. It will also be convenient to relabel the unbalanced parts of the transition rates (5.10) according to

$$\Delta_q \quad \text{with} \quad 1 \leqslant q \leqslant Q. \tag{5.12}$$

The simplest situation is provided by $Q = 1$. In this case, rule 1 leads to

$$J_{\text{tot}}(\Delta_1, F) = \frac{a_0(F) + a_1(F)\,\Delta_1}{b_0(F) + b_1(F)\,\Delta_1} \tag{5.13}$$

with $a_0(F = 0) = 0$ as follows from rule 6.

For $Q = 2$, the dependence of the total current on the unbalanced rate constants Δ_1 and Δ_2 has the general form

$$J_{\text{tot}}(\Delta_1, \Delta_2, F) = \frac{a_0 + a_1\Delta_1 + a_2\Delta_2 + a_{12}\Delta_1\Delta_2}{b_0 + b_1\Delta_1 + b_2\Delta_2 + b_{12}\Delta_1\Delta_2} \tag{5.14}$$

where all coefficients a and b again depend on the external force F with $a_0 = 0$ for $F = 0$.

Likewise, for $Q \geqslant 3$, rule 1 implies that the total current $J_{\text{tot}}(\Delta_1, \ldots, \Delta_Q)$ is given by the ratio of two *multilinear polynomials, the degree of which is bounded from above* both by Q and by $K(M-1)$,[3] and rule 6 leads to $a_0 = 0$ for $F = 0$.

The generic features just described are valid for an arbitrary number of balanced transitions. Thus, we could add more and more balanced transitions in order to attain balanced rate functions $\Omega^{db}_{mn}(x)$ which vary continuously with x. This implies that the generic current-rate relationships should also be valid for transition rate functions

$$\Omega_{mn}(x) = \Omega^{db}_{mn}(x) + \sum_q \Delta_q \ell_\Omega \delta(x - x_q) \tag{5.15}$$

where the functions $\Omega^{db}_{mn}(x)$ satisfy detailed balance but have an otherwise arbitrary x-dependence and the summation over q depends on the level pair (m, n).

On the other hand, if one studies ratchets for which the unbalanced parts of the transition rate functions $\Omega_{mn}(x)$ are described by continuously varying functions, one obtains a stochastic resonance and the total current exhibits a maximum at sufficiently large transition rates.[8, 7] In the context of the stochastic network considered here, this would correspond to the limit of large Q.

The current-rate relationships discussed so far represent the most general forms consistent with a given value of Q. If the network exhibits

[3] In general, Q may exceed $K(M-1)$. In this case, one must have unbalanced transitions which emanate from the same vertex or which correspond to l-cycles in the network. Such transitions can contribute to the total current via different s-cycles.

some additional constraints or symmetries, some of the F-dependent polynomial coefficients will be identically zero. One example is provided by $Q = 2$ with two unbalanced transitions which emanate from the same vertex (k, m). In this case, one has $a_{12} = b_{12} = 0$ in (5.14) as follows from rule 3. Another example is provided by the *strongly unbalanced limit* in which one ignores all balanced transitions. In this limit, both relationships (5.13) and (5.14) simplify since rule 2 implies that the zeroth order coefficients a_0 and b_0 vanish for all F while the first order coefficients a_1 and a_2 now vanish for $F = 0$ as follows from rule 6.

5.3. Other Types of Networks

Since the ratchet models considered here are equivalent to the networks introduced in Section 3 and displayed in Fig. 1, the above classification scheme for the rate dependence of the total current also applies to these networks. As mentioned, any (finite) lattice in $(1+d_\perp)$ dimensions can be mapped onto such a network.

It is interesting to note, however, that these networks need not be as regular as in Fig. 1. Indeed, each such network is completely defined by its graph, i.e., by the set of its vertices and by the pairs of di-edges which connect these vertices. Thus, we can distort the network shown in Fig. 1 in an arbitrary way and still get the same classification for the relationship between the total current and the unbalanced rates. Likewise, starting from a regular network as in Fig. 1 but for large values of K and M, we can eliminate many of the pairs of di-edges by setting the corresponding transition rates equal to zero. In this way, we can obtain networks of completely different "shapes."

The only constraint which is essential are the periodic boundary conditions which imply that the vertex $(k = 1, m)$ is directly connected, by a pair of di-edges, to the vertex $(k = K, m)$ for all values of m. Between these two "slices" at $m = 1$ and $m = M$, one can then have many kinds of different networks. In particular, it is not difficult to see that these networks may contain unbalanced transitions corresponding to di-edges which run parallel to the x-coordinate.

6. UNIVERSAL FEATURES OF MOTOR VELOCITY

Finally, let us return to the problem of molecular motors for which the total current $J_{\rm tot}$ determines the motor velocity v via $v = \ell J_{\rm tot}$. In this case, the number Q of unbalanced transitions is equal to the number of possible catalytic steps per motor cycle. In order to estimate this number for a specific motor, one should focus on its catalytic domains or heads.

Conventional kinesin, for example, has two heads and a long tail. Since we are not interested in the various conformations of this tail, we want to focus on a two-headed kinesin which walks in a processive way but has the shortest possible tail.[4] As such a motor walks along the filament, it will undergo many balanced and a few unbalanced transitions as explained next.

6.1. Balanced Versus Unbalanced Transitions

Thus, let us imagine to watch the motor protein and the filament with a rather high resolution. Since we use the context of classical statistical mechanics, the resolution cannot become arbitrarily high, but we could imagine to resolve structures of the order of a few angstroms. On such a scale, we would see small groups of atoms which are expected to behave classically, i.e., we could presumably describe the movements of these groups by position and momentum variables. Now, most of the motion which we would observe on this scale is due to thermal fluctuations which satisfy detailed balance since our systems have constant temperature and pressure.

The molecular motor cycle contains several adsorption and desorption processes. First, one head of the motor molecule may bind to and unbind from the filament. Likewise, ATP can bind to one of the heads, and ADP and/or the phosphate ion (P_i) can unbind from such a head after the hydrolysis. In general, the reverse processes of ATP unbinding and ADP binding are possible as well. If we replace ATP by a nonhydrolyzable analogue such as AMP-PNP, we suppress the hydrolysis step of the motor cycle, and all of these adsorption and desorption processes correspond to balanced transitions. From this point of view, the only processes which should be described by *un*balanced transitions are chemical reaction steps at which a chemical or covalent bond is broken or reshuffled.

For cytoskeletal motors, this chemical reaction is provided by the hydrolysis of ATP which can be summarized by the reaction scheme

$$\mathrm{ATP} \rightleftharpoons \mathrm{ADP} + \mathrm{P_i} \tag{6.1}$$

where P_i denotes the phosphate ion. In chemical kinetics, one introduces two reaction rate constants, κ_1 and κ_2, and assumes that chemical *equilibrium* is reached as soon as

$$\kappa_1 \Gamma_{\mathrm{ATP}} = \kappa_2 \Gamma_{\mathrm{ADP}} \Gamma_{\mathrm{P}} \tag{6.2}$$

[4] Kinesin seems to be characterized by a long-ranged interaction between the tail and the motor domains since the tail blocks the catalytic activity if it is not bound to some cargo.[38] This regulation mechanism is not included in our models.

where Γ_{ATP}, Γ_{ADP}, and Γ_{P} are the concentrations of the three molecular species. In the framework considered here, the state of the motor before and after the hydrolysis corresponds to two states (k, m) and (k, n). Thus, in order to describe the deviation from equilibrium and detailed balance, it seems natural to define the unbalanced parts of the hydrolysis step via the transition rates

$$\Delta_{mn}(x_k) = e^{V_m(x_k)}\kappa_1(F)\,\Gamma_{\mathrm{ATP}} \equiv \hat{\kappa}_1(F)\,\Gamma_{\mathrm{ATP}} \tag{6.3}$$

and

$$\Delta_{nm}(x_k) = e^{V_n(x_k)}\kappa_2(F)\,\Gamma_{\mathrm{ADP}}\Gamma_{\mathrm{P}} \equiv \hat{\kappa}_2(F)\,\Gamma_{\mathrm{ADP}}\Gamma_{\mathrm{P}} \tag{6.4}$$

between these two motor states. As indicated, the reaction rate constants will, in general, depend on the external force F.

In typical motor experiments, one usually starts from the situation in which one has a relatively large concentration of ATP but (almost) no ADP. If these systems contain only a small number of motors, they are well separated from the state of chemical equilibrium over the accessible time scales of the experiments. In this limit of small Γ_{ADP}, one may use

$$\Delta_{mn}(x_k) = \hat{\kappa}_1(F)\,\Gamma_{\mathrm{ATP}} \qquad \text{and} \qquad \Delta_{nm}(x_k) \approx 0. \tag{6.5}$$

In the literature on cytoskeletal motors, the ATP hydrolysis contained in the motor cycle is often described by several substeps. As an example, consider one motor domain of two-headed kinesin (K) bound to a microtubule (M). This bound state is believed to be rather stable until an ATP molecule arrives and binds to K. The bound K/ATP then leads to the hydrolysis step as given by (6.1) after which $\mathrm{P_i}$ and ADP unbind from K. Thus, one has the sequence $\mathrm{M/K + ATP \rightarrow M/K/ATP \rightarrow M/K/ADP/P_i \rightarrow M + K/ADP + P_i}$. The latter sequence is typically assumed to follow Michaelis–Menten kinetics[39] which implies that the corresponding unbalanced transition rate $\Delta_{mn}(x_k)$ is given by[1, 2]

$$[\Delta_{mn}(x_k)]^{-1} = [\tilde{\kappa}_1(F)\,\Gamma_{\mathrm{ATP}}]^{-1} + [\tilde{\kappa}_2(F)]^{-1} \tag{6.6}$$

with reaction rate constants $\tilde{\kappa}_1$ and $\tilde{\kappa}_2$ which again may depend on the external force F.

In principle, the molecular motor could contain allosteric domains which bind regulatory molecules. The transition rate $\Delta_{mn}(x_k)$ could then exhibit a sigmoidal dependence on Γ_{ATP} as found for allosteric enzymes.[39, 2]

6.2. Rate Dependence of Motor Velocity

We can now combine the general relationships between the total current J_{tot} and the unbalanced transition rates as described in Section 5 with the specific forms for these unbalanced rates as discussed in the previous subsection. In this way, we obtain the functional dependence of the motor velocity $v = \ell J_{\text{tot}}$ on the ATP concentration and on the external force. As for the current-rate relationships, this functional dependence is primarily determined by the total number Q of unbalanced transitions per motor cycle. In order to simplify the discussion, we will implicitly assume that both K and M are large and that $Q \leqslant K(M-1)$.

If the motor has a single head, one expects to have only one hydrolysis step per motor cycle which implies $Q = 1$. If the motor has two identical heads, one will have $Q = 2$ if *both* heads must be in a unique conformational state in order to have an ATP hydrolysis reaction at *one* of these heads.

In general, one would expect that each head of a two-headed motor should have a unique state in order to become catalytic, but the second head may still have some conformational freedom. If one head can be active for two or three different conformations of the other head, one has $Q = 4$ or $Q = 6$, respectively. If the two heads are not identical as applies, e.g., to certain kinesin constructs, one could also imagine motor cycles characterized by $Q = 3$ or $Q = 5$.

For a certain value of Q, the models considered here lead to a certain rate dependence of the total current as described in Section 5.2. Using the dependence of the unbalanced transition rates $\Delta_{mn}(x_k)$ on the various concentrations and on the external force F as discussed in Section 6.1, one then obtains a certain dependence of the motor velocity on these control parameters.

In our previous work, the unbalanced transition rates were taken to have the Michaelis–Menten form as given by (6.6). One then obtains the general functional relationships as given by[2]

$$v(\Gamma, F) = \left[\sum_{n=0}^{Q} g_n(F)\, \Gamma^n \right] \Big/ \left[\sum_{n=0}^{Q} h_n(F)\, \Gamma^n \right] \tag{6.7}$$

with $\Gamma = \Gamma_{\text{ATP}}$ and $g_0(F=0) = 0$ (and $Q \leqslant K(M-1)$ was implicitly assumed). Thus, the velocity can be expressed in terms of the ratio of two Γ-polynomials of degree Q with F-dependent coefficients. The same functional relationships are obtained if one uses the somewhat different parametrization of the unbalanced transition rates as given by (6.5).

In this way, one arrives at a general classification scheme for the functional dependence of the velocity on the *two* parameters Γ and F which

agrees, for $Q = 1$, with the experimental observations on kinesin as described by (1.1). For each value of Q, the functional relationships as given by (6.7) are *universal* in the sense that they are valid (i) for any number of balanced transition rates, (ii) for any choice of the molecular force potentials, (iii) for arbitrary load force F, and (iv) for any force dependence of the Michaelis–Menten reaction rate constants $\tilde{\kappa}_1(F)$ and $\tilde{\kappa}_2(F)$ in (6.6) or of the reaction rate constant $\hat{\kappa}_1(F)$ in (6.5).

As mentioned in Section 5.2, the current-rate relationships simplify if some of the polynomial coefficients vanish for all F because of some additional constraint of symmetry. Likewise, some of the polynomial coefficients $g_n(F)$ and $h_n(F)$ in (6.7) may vanish for all F. This happens, e.g., for models with $(K, M) = (2, 2)$ and $(K, M) = (2, 3)$ in the strongly unbalanced limit with $Q = 4$ as studied for kinesins with two identical heads.[1] This reduction in the polynomial degree is related to the symmetry between the two identical heads. Since this symmetry is absent for kinesin constructs which have two different heads, our theory predicts that the corresponding velocity-rate relationship will also be different.

Finally, if one uses the unbalanced transition rates as given by (6.3) and (6.4), our theory makes some definite predictions about the dependence on the ADP and P_i concentrations which should be accessible to experiments.

ACKNOWLEDGEMENTS

R.L. takes this opportunity to thank Michael E. Fisher for much advice and inspiration during many years of stimulating interactions.

GLOSSARY: LIST OF SYMBOLS

All symbols are treated as words which are ordered alphabetically.

d	spatial dimensionality
D_m	diffusion coefficient in lateral currents J_m
F	applied (tangential) force; a load force corresponds to $F < 0$
Γ	concentration of fuel molecules such as ATP
Γ_*	characteristic intermediate concentration
I_m	transition current density for internal state m
J_m	lateral current for internal state m
$J_{\rm tot}$	total lateral current
K	number of locations for transitions between internal states
ℓ_Ω	molecular "localization" length for transitions rates
ℓ	period of molecular force potentials

M	number of internal motor states
P_m	probability density for internal state m
P_{tot}	total or position probability density
Ω_{mn}	spatially dependent transition rate function from state m to state n
ω_{mn}	transition rate from state m to state n
x	spatial coordinate for motor position
x_k	position at which motor undergoes localized transition
t	time
T	temperature in energy units
U_m	molecular force potential for internal state m
V_m	effective force potential as defined in (2.2).
v	motor velocity

REFERENCES

1. R. Lipowsky and T. Harms, *Eur. Biophys. J.* **29**:542 (2000).
2. R. Lipowsky, *Phys. Rev. Lett.* **85**:4401 (2000).
3. R. Lipowsky, in *Stochastic Processes in Physics, Chemistry and Biology*, Lecture Notes in Physics, Vol. 557, J. A. Freund and T. Pöschel, eds. (Springer, Heidelberg, 2000), pp. 21–31.
4. N. van Kampen, *Stochastic Processes in Physics and Chemistry* (Elsevier, Amsterdam, 1992).
5. R. Astumian and M. Bier, *Phys. Rev. Lett.* **72**:1766 (1994).
6. J. Prost, J.-F. Chauwin, L. Peliti, and A. Ajdari, *Phys. Rev. Lett.* **72**:2652 (1994).
7. T. Harms and R. Lipowsky, *Phys. Rev. Lett.* **79**:2895 (1997).
8. F. Jülicher, A. Ajdari, and J. Prost, *Rev. Mod. Phys.* **69**:1269 (1997).
9. A. Parmeggiani, F. Jülicher, A. Ajdari, and J. Prost, *Phys. Rev. E* **60**:2127 (1999).
10. J. Howard, A. J. Hudspeth, and R. D. Vale, *Nature* **342**:154 (1989).
11. K. Svoboda, C. Schmidt, B. Schnapp, and S. Block, *Nature* **365**:721 (1993).
12. K. Svoboda and S. Block, *Cell* **77**:773 (1994).
13. M. J. Schnitzer and S. M. Block, *Nature* **388**:386 (1997).
14. W. Hua, E. C. Young, M. L. Fleming, and J. Gelles, *Nature* **388**:390 (1997).
15. W. O. Hancock and J. Howard, *J. Cell Biol.* **140**:1395 (1998).
16. M. Thormählen *et al.*, *J. Mol. Biol.* **275**:795 (1998).
17. S. Gilbert, M. Moyer, and K. Johnson, *Biochemistry* **37**:792 (1998).
18. K. Visscher, M. J. Schnitzer, and S. M. Block, *Nature* **400**:184 (1999).
19. Y. Okada and N. Hirokawa, *Science* **283**:1152 (1999).
20. A. Mehta *et al.*, *Nature* **400**:590 (1999).
21. M. Rief *et al.*, *Proc. Nat. Acad. Sci. USA* **97**:9482 (2000).
22. A. Mehta, *J. Cell Sci.* **114**:1981 (2001).
23. Z. Wang and M. Sheetz, *Biophys. J.* **78**:1955 (2000).
24. S. King, *Biochimica Biophysica Acta - Mol. Cell Res.* **1496**:60 (2000).
25. E. Hirakawa, H. Higuchi, and Y. Toyoshima, *Proc. Nat. Acad. Sci. USA* **97**:2533 (2000).
26. M. E. Fisher and A. B. Kolomeisky, *Proc. Natl. Acad. Sci. USA* **98**:7748 (2001).
27. A. Kolomeisky and B. Widom, *J. Stat. Phys.* **93**:633 (1998).
28. M. E. Fisher and A. Kolomeisky, *Proc. Natl. Acad. Sci. USA* **96**:6597 (1999).
29. N. Jaster and R. Lipowsky, to be published.

30. D. Keller and C. Bustamante, *Biophys. J.* **78**:541 (2000).
31. H. Risken, *The Fokker–Planck Equation: Methods of Solution and Applications* (Springer Verlag, Berlin, 1989).
32. A. Ajdari, *Europhys. Lett.* **31**:69 (1995).
33. R. Lipowsky, S. Klumpp, and T. Nieuwenhuizen, *Phys. Rev. Lett.* **87**:108101/1 (2001).
34. R. Lipowsky, in *Biological Physics 2000*, V. Sa-yakanit, L. Matsson, and H. Frauenfelder, eds. (World Scientific, New Jersey, 2001), pp. 41–56.
35. T. Nieuwenhuizen, S. Klumpp, and R. Lipowsky, *Europhys. Lett.* **58**:468 (2002).
36. W. D. Wallis, *A Beginner's Guide to Graph Theory* (Birkhäuser, Boston, 2000).
37. J. Howard, *Mechanics of Motor Proteins and the Cytoskeleton*, first edn. (Sinauer, New York, 2001).
38. D. Hackney, *Nature* **377**:448 (1995).
39. A. Lehninger, D. Nelson, and M. Cox, *Principles of Biochemistry*, 2nd edn. (Worth Publishers, New York, 1993).